Applied Radiation and Isotopes 149 (2019) 38–47

Contents lists available at ScienceDirect

Applied Radiation and Isotopes

journal homepage: www.elsevier.com/locate/apradiso

A new application of radioactive particle tracking using MCNPX code and artificial neural network

Roos Sophia de F. Dam[a], Tâmara P. Teixeira[a], William L. Salgado[a], César M. Salgado[a,*]

[a] Instituto de Engenharia Nuclear (IEN / CNEN – RJ), Rua Hélio de Almeida 75, 21941-906, Cidade Universitária, RJ, Brazil

HIGHLIGHTS

- Radioactive Particle Tracking methodology developed using MCNPX code.
- The detection system uses ^{137}Cs (662 keV) gamma-ray source and eight NaI(Tl) detectors.
- An artificial neural network gives the position of the radioactive particle.

ARTICLE INFO

Keywords:
Gamma densitometry
MCNPX code
Artificial neural network
NaI(Tl) scintillator detector
Radioactive particle tracking

ABSTRACT

Stirrers and mixers are highly used in chemical, food, pharmaceutical, cosmetic, concrete industries and others. During the fabrication process, the equipment may fail to appropriately stir or mix the solution. Besides that, it is also important to determine when the right homogeneity of the mixture is attained. Thus, it is very important to have a diagnosis tool for these industrial units to assure the quality of the product and maintain market competitiveness. Nuclear techniques, such as gamma densitometry, are widely used in industry to overcome a sort of difficulties, as they are minimally non-invasive techniques. This paper presents a method based on the principles of the radioactive particle tracking technique to predict the instantaneous position of a radioactive particle to monitor a concrete mixture inside an industrial unit by means of Monte Carlo method and artificial neural network. Counts obtained by an array of detectors properly positioned around the mixing canister will be correlated to each other, by means of an appropriate mathematical search location algorithm, in order to predict the instantaneous positions occupied by an inserted radioactive particle. The simulation consists of a detection geometry of eight NaI(Tl) scintillator detectors, a 662 keV ^{137}Cs point source with isotropic emission of gamma-rays and a polyvinyl chloride tank. At first, the tank is air filled and, afterwards, filled with concrete made with Portland cement. The modeling of the detection system is performed using the MCNPX code. For both medium, the correlation coefficient was 0.99 for all coordinates, which indicates that this methodology could be a good tool to evaluate industrial mixers.

1. Introduction

Stirrers and mixers are highly used in the industry for processes such as dispersion and homogenization. Several industrial segments need this type equipment, such as chemical, food, pharmaceutical, concrete and cosmetic industries. The concrete industry, for example, aims to obtain homogeneous mixtures with specific properties for drying time, adhesion and hardening for building foundations, waterproofing surfaces and regularize walls and floors. Stirrers are designed for each application with specific configurations, depending on the desired characteristics, such as density, phase and viscosity of the product. It is important to verify the appropriate functioning of the equipment and the stirring or mixing procedure to attain good homogeneity of the mixture. The proposed method intends to fulfill the needs for adequate quality control of the fabrication process and final product.

Although conventional sensors can be used, they are invasive and have high installation costs. Nuclear techniques, such as radioactive particle tracking (RPT), are widely used in industry to overcome some difficulties, as they are non-invasive techniques, such as obtaining flow field information about solid-phase motion in fluidized beds (Larachi et al., 1994) and to reconstruct online flow visualization in multiphase reactors (Godfroy et al., 1997), among others.

* Corresponding author.
E-mail addresses: rsophia.dam@gmail.com (R.S.d.F. Dam), tamarateixeira.eng@gmail.com (T.P. Teixeira), william.otero@hotmail.com (W.L. Salgado), otero@ien.gov.br (C.M. Salgado).

https://doi.org/10.1016/j.apradiso.2019.04.011
Received 21 November 2018; Received in revised form 11 February 2019; Accepted 5 April 2019
Available online 10 April 2019
0969-8043/

RPT consists of monitoring a radioactive particle inside a volume of interest, in this work this volume is represented by a tank with concrete. To track the particle, it is necessary to have a detection system composed by an array of radiation detectors. It is important to note that the radioactive particle must have the same characteristics of the fluid where it is inserted.

The instantaneous particle position is calculated through a reconstruction algorithm that converts the detector counts as a function of coordinates of the particle. Many reconstruction algorithms have been developed, such as a weighted regression scheme (Devanathan et al., 1990), a modified weighted regression scheme (Luo et al., 2003), the cross correlation technique (Bhusarapu et al., 2005); the Monte Carlo approach (Blet et al., 2000; Doucet et al., 2008; Larachi et al., 1994; Roy et al., 2002; Mosorov and Abdullah, 2011; Yunos et al., 2018) and feedforward artificial neural network (Godfroy et al., 1997).

Artificial neural networks (ANN) (Rumelhart and McClelland, 1986; Haykin, 1999) have been used for some decades in different fields of study. With an ANN it is possible to study and reconstruct online flow visualization in multiphase reactors (Godfroy et al., 1997), study the chaotic behavior of a three-phase fluidized bed (Otawara et al., 2002), predict volume fractions in multiphase flows (Salgado et al., 2009, 2010) and identify flow regime (Salgado et al., 2010).

This study consists of the modeling of a setup with eight NaI(Tl) scintillator detectors placed in two planes on the z-axis, a ^{137}Cs point source with isotropic gamma-ray emission and a polyvinyl chloride (PVC) tank filled with concrete that is made with Portland cement. The Monte Carlo method is used to model the detection system and the simulations are provided by means of the Monte Carlo N-Particle eXtended (MCNPX) computer code (Pelowitz, 2005). The reconstruction algorithm used is given by a 3-layer feedforward ANN with a backpropagation algorithm (Werbos, 1974; Parker, 1985; Rumelhart and McClelland, 1986; Chauvin and Rumelhart, 1995) to calculate the instantaneous position of the radioactive particle. Dam and Salgado (2017) started this study using an air-filled tank to show the potentiality of the MCNPX code and the ANN. In this paper, the results has a superior design of some parameters of the ANN such as learning rate, momentum, activation functions and number of neurons. Besides that, the addition of a tank filled with concrete, made with Portland cement, to evaluate a concrete mixer. Thus, the aim of this study is to use MCNPX code to feed an ANN that was used as a reconstruction algorithm to track a radioactive particle in a concrete mixer.

2. Theoretical foundations

2.1. Principles of the radioactive particle tracking (RPT)

Gamma rays are highly penetrating electromagnetic radiation that can travel long distances before an interaction occurs. In addition to other parameters, the number of photons recorded by a gamma radiation detector depends on the distance between the gamma ray source and the detector. This is the basic principle explored in the radioactive particle tracking technique, which uses an array of radiation detectors, generally scintillator detectors, to identify the location of a single radioactive particle. It is important to highlight that the radioactive particle must have identical physical characteristics to the fluid investigated inside the volume of interest.

The determination of the coordinates (x, y, z) of the radioactive particle is given by algorithms based on phenomenological or empirical approaches, which consider the relation between the number of photons recorded by each of the detectors and the location of the particle. The counts registered in each detector during a time interval is expressed by Equation 1 (Tsoulfanidis, 1983).

$$C_i = t \cdot I(\%) \cdot A \cdot r \cdot \varepsilon_i \quad \rightarrow \quad i = 1, \ldots, n$$

Where t is the live time interval, A is the source activity, I (%) is the number of photons emitted by disintegration, r is true net counting rate per second and ε_i is the efficiency of ith detector. Besides the distance to the particle, the number of photons recorded depends on the attenuation properties of the materials in between the particle and the detector, and on the properties of the detector itself (Chaouki et al., 1997). For a greater accuracy in particle location, a large number of detected photons is required due to the counting statistical fluctuations.

The type of the detectors used depends on some aspects that affect the interaction of the gamma-rays with the detector materials (Chaouki et al., 1997). The most important aspects are the characteristics of the radioactive particle such as gamma-ray energy and activity; the types of gamma-rays interaction with matter (for this work only photoelectric effect and Compton scattering are important); the solid angle at which the irradiated surface of the detector is subjected; the detection efficiency; the photopeak area and; the dead-time of the acquisition system.

2.2. MCNPX code

The Monte Carlo computer code N-Particle eXtended (MCNPX) considers the effects of the interaction of radiation with matter with thirty different particles and four light ions (Pelowitz, 2005).

The MCNPX code allows the construction of complex, three-dimensional geometries, serving as a tool of extreme relevance for modeling nuclear installations, radiation detectors, shielding studies and other applications. Because it is a well-founded and validated code, its results and calculation methodology are widely accepted.

In this work, the MCNPX computer code was used to establish the appropriate geometry to be used in RPT, determining the positioning of the detectors, the characteristics of the radioactive particle and the fluid inside the tank. In addition, the results obtained with the code were used to feed the ANN.

2.3. Artificial neural network

An artificial neural network (ANN) is a mathematical model inspired by the human neuronal function. In this way, its most important characteristic is to learn through examples (Haykin, 1999). If an appropriate set of data is given to the ANN, it is able to recognize patterns, generalizing knowledge during the learning process, that is, ANN is able to assign a response to situations that are not included in the training set. There are two phases of the ANN:

i. Training phase or learning process: This is where the ANN is supposed to learn and recognize patterns by using a learning algorithm. It is often an offline phase.
ii. Working phase: The trained ANN is used to respond to new situations. It is the online phase.

3. Methodology

The methodology described in this work requires a great number of measurements to perform the ANN training. In this way, the MCNPX code was used to overcome this difficulty. In this section, it will be described the simulated geometry using the MCNPX code and the method used to predict the radioactive particle position inside the volume of interest. The calculation of the instantaneous particle position was made with a location algorithm by an ANN.

3.1. Simulated geometry

The geometry simulation was performed with the MCNPX code; it consists of a PVC tank with 9.5 cm of inner radius and 100 cm of length. The PVC tank was filled with two different materials, in two distinct moments: air (density = 1.205E-3 g cm^{-3}) and concrete (density = 2.3 g cm^{-3}). It is important to mention that the tank filled with air was used to evaluate the potential of the ANN training using the

Table 1
Weight fractions of the materials.

Elements	Air	Concrete
C	0.000124	0.001000
N	0.755268	–
O	0.231781	0.529107
Ar	0.012827	–
H	–	0.010000
Na	–	0.016000
Mg	–	0.002000
Al	–	0.033872
Si	–	0.337021
K	–	0.013000
Ca	–	0.044000
Fe	–	0.014000

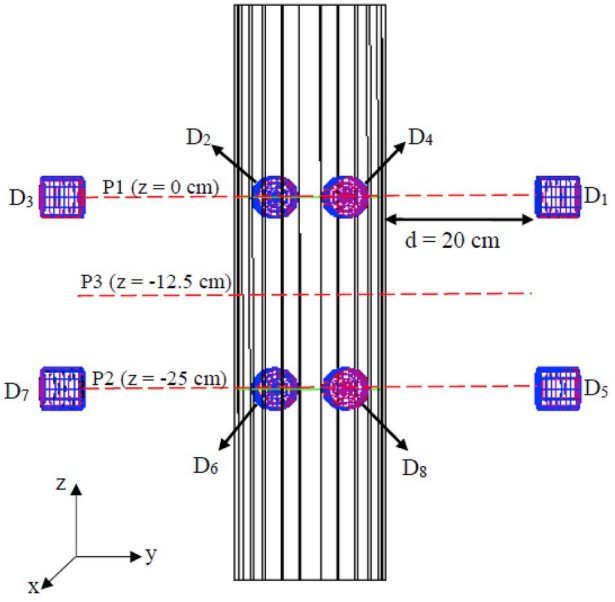

Fig. 1. Geometry simulated with MCNPX code.

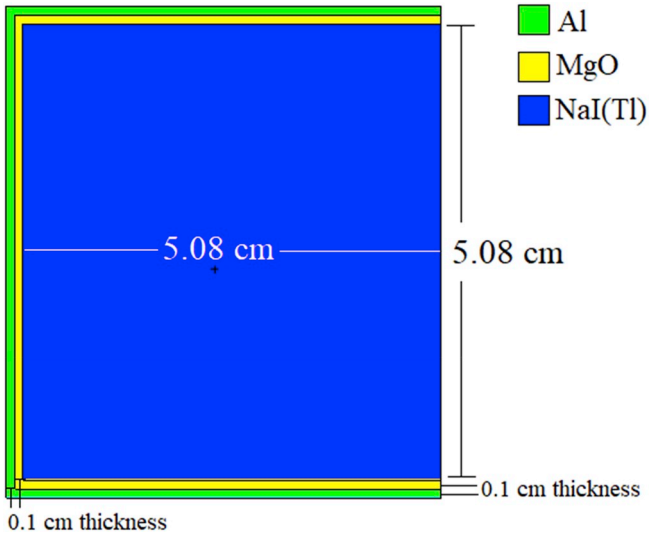

Fig. 2. The modeling of the scintillator detector in details.

results from the MCNPX computer code. Depending on the application, for very dense materials, it might be necessary to use a gamma-ray source of higher energy because of the attenuation properties.

The weight fractions of the materials are presented in Table 1

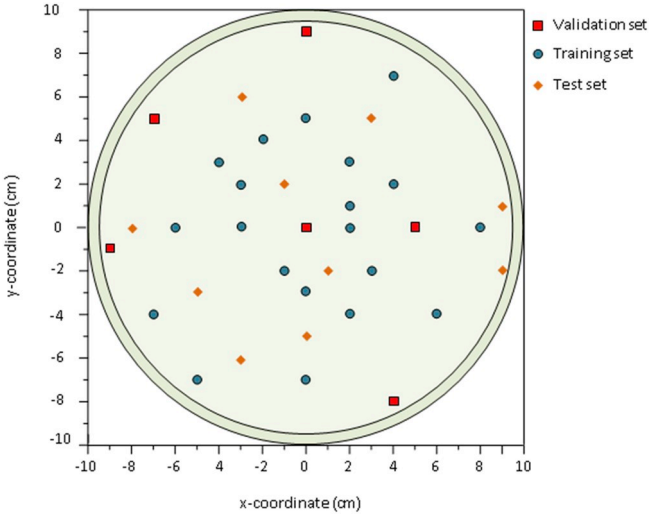

Fig. 3. Coordinates x and y for training, test and validation sets for plane P1.

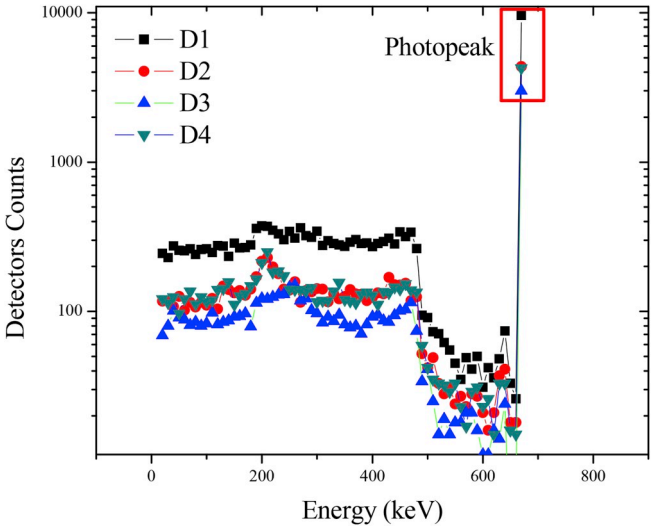

Fig. 4. PHD of four detectors highlighting the photopeak area used as inputs of the ANN.

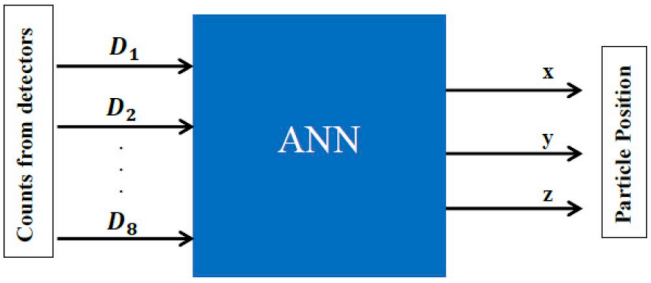

Fig. 5. ANN structure.

(McConn et al., 2011). The radioactive particle is a 662 keV point source with isotropic emission of gamma rays. On the outer side of the tank, eight 2″x2″ cylindrical NaI(Tl) detectors were placed in two planes perpendicular the z-axis at positions 0 cm, plane P1, and -25 cm, plane P2. The tank represents a simplified model of a stirrer, as shown in Fig. 1.

Planes P1 and P2 have four NaI(Tl) detectors each, placed across each other in a 90° angle. The distance between the detectors and the tank is 20 cm. The simulated detectors consist of a NaI(Tl) crystal,

Table 2
Parameters used for ANN training.

Learning rate η = 0.01 – Momentum = 0.1					
PARAMETERS	Layers				
	Input	Hidden			Output
Activation Functions	Linear [-1,1]	Gaussian	Tanh	Gaussian-complement	Logistic
Neurons	8	4	4	4	3

surrounded by a reflective layer composed of magnesium oxide (MgO) and an outer aluminum layer (Al). The MgO and Al layers have 0.1 cm thickness at the front and on the side. Fig. 2 shows details of the modeling of the detector (side view). It is necessary to emphasize that the photomultiplier was not simulated in this work.

In the MCNPX code input file, through the tally card F8, the response of the simulation is the pulse height distribution (PHD). In the simulation, the results are normalized to the source activity in number of photons. The number of counts registered by each detector is given by Equation 1 (Section 2.1). The simulated detectors respond well in the photopeak region for 662 keV and this part of the spectrum is well characterized, therefore, in this work, only the region corresponding to the photoelectric absorption was used for the ANN training. To ensure that the relative error remains below 5% in the photopeak region, it was used 1E7 as number of histories (NPS) in the simulations. Considering the frontal and side distance between the source and the detector, the absolute efficiency was evaluated. All detectors have the same efficiency curve and the energy resolution was not relevant for this work.

3.2. Artificial neural network (ANN) training

The principle of the RPT technique is to correlate each detector counting to the instantaneous particle position inside the volume of interest. In this work, the instantaneous position of the particle is calculated by a location algorithm given by a 3-layer feed-forward multilayer perceptron with the backpropagation algorithm.

To ensure a properly working neural network, it is necessary a training, a test and a validation set to evaluate the offline phase of the ANN. The test subset is used to evaluate the ANN generalization and to avoid the overtraining. These sets were chosen in a certain proportion, which are: 60% training, 30% test and 10% validation (Zadeh et al., 2016). Data sets were distributed empirically.

The radioactive particle was positioned in 108 different positions (x,y,z) in the planes P1 and P2, mentioned before, and a third plane at −12.5 cm (P3). All these positions were distributed evenly in the region of interest. In the plane P1, the x and y coordinates range was sampled from −9 to 9 cm. These positions were replicated in the planes P2 and P3. The z-coordinate was varied in three positions (z = 0 cm, z = −12.5 cm and z = −25 cm). Fig. 3 shows the x and y coordinates for plane P1 (36 positions). These ranges were chosen so that the radioactive particle was inside the simulated tank.

ANN training patterns are composed by inputs and outputs. Inputs

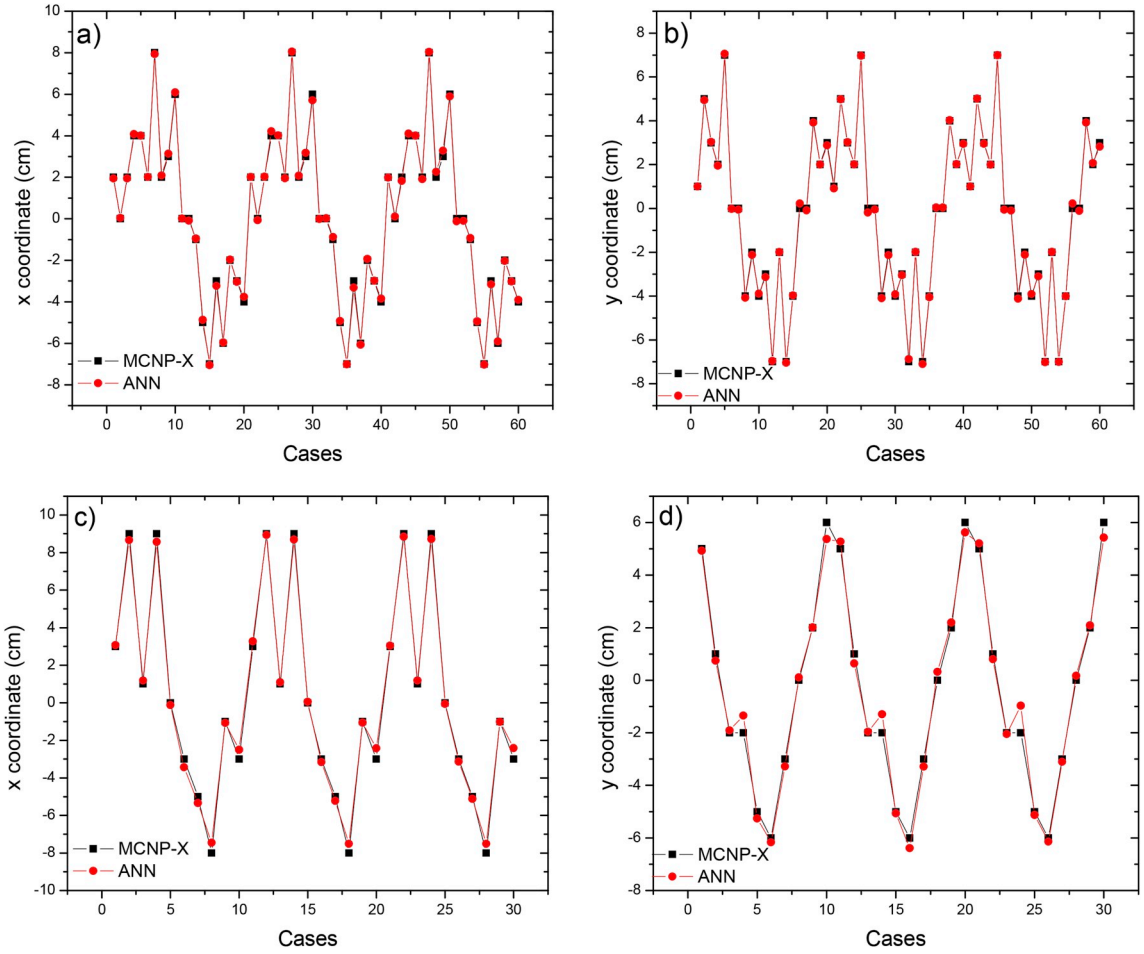

Fig. 6. Results for the air filled tank comparing MCNPX with ANN: a) x-coordinate of training set; b) y-coordinate of training set; c) x-coordinate of test set; d) y-coordinate of test set.

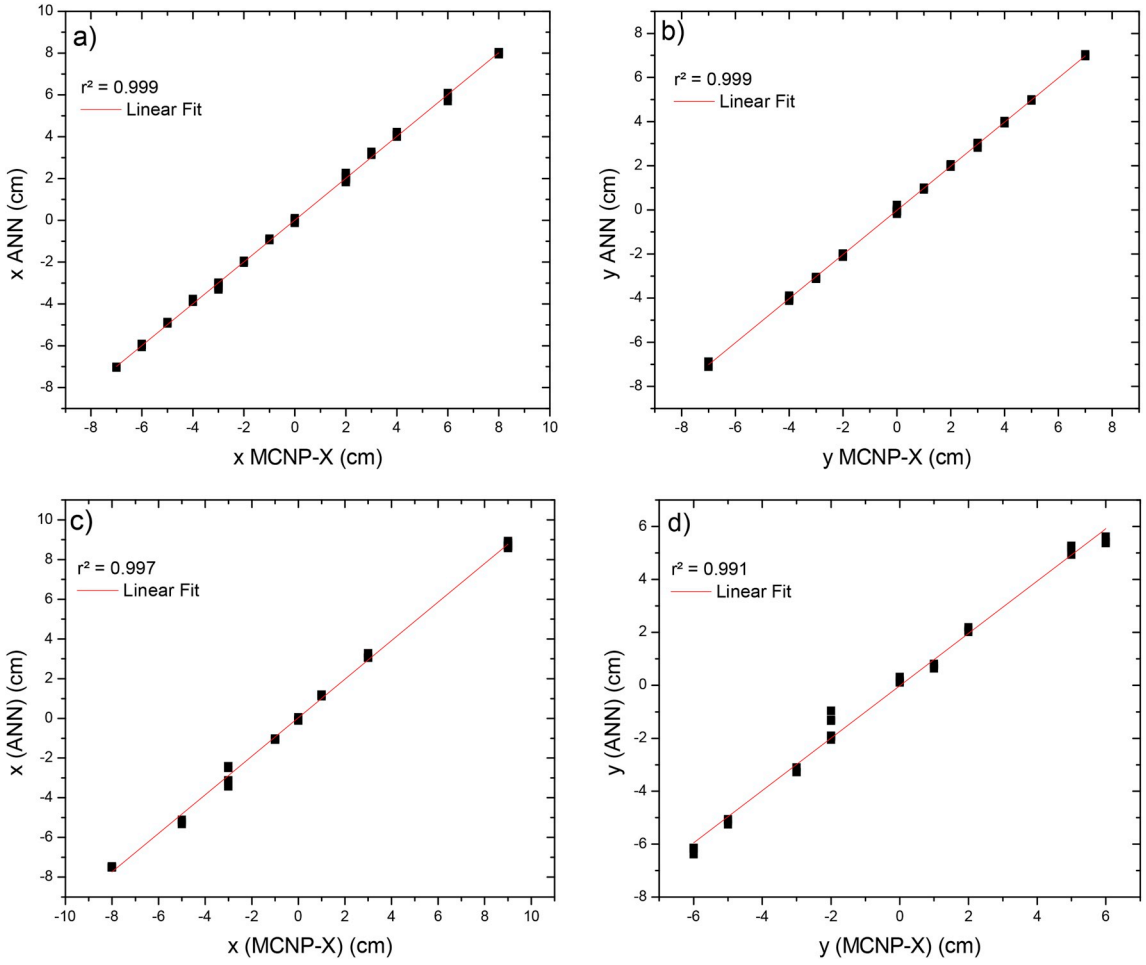

Fig. 7. Linear fit results for the air filled tank: a) x-coordinate of the training set; b) y-coordinate of the training set; c) x-coordinate of the test set; d) y-coordinate of the test set.

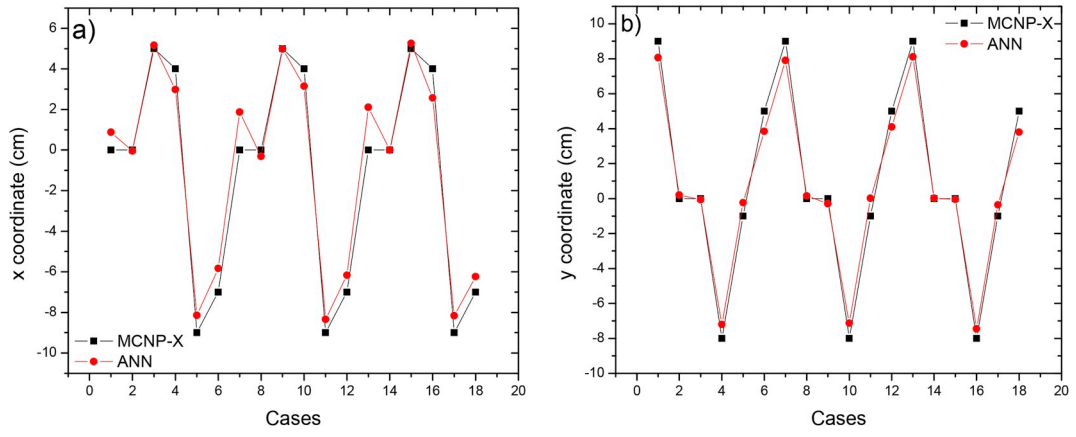

Fig. 8. Results of the validation set for the air filled tank comparing MCNPX with ANN for: a) x-coordinate; b) y-coordinate.

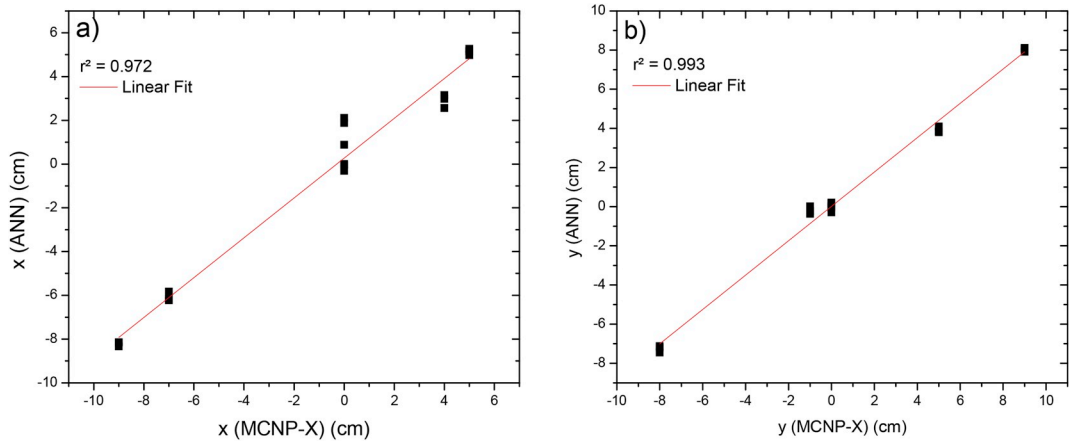

Fig. 9. Linear fit results of the validation set for the air filled tank: a) x-coordinate; b) y-coordinate.

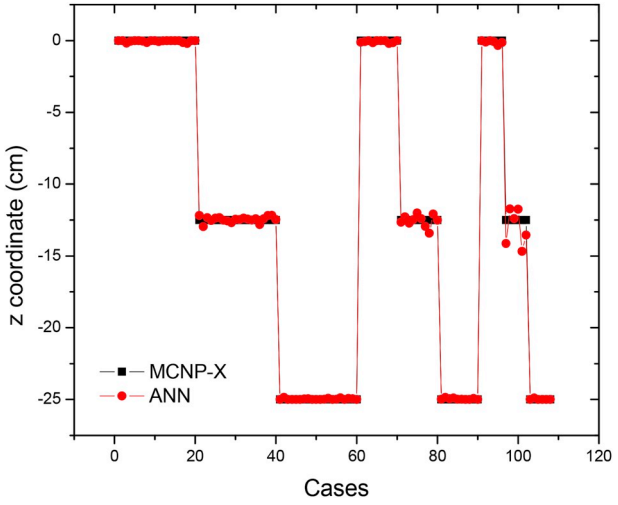

Fig. 10. Results of the z-coordinate for training, test and validation sets for the air filled tank.

Table 3
Processed data from the trained ANN for the air filled tank.

Processed data	Coordinates		
Relative Error	x	y	z
< 5%	60.00	63.23	91.67
5%–10%	23.33	18.38	5.55
10%–20%	13.33	6.90	2.78
20%–30%	2.22	3.45	0
> 30%	1.12	8.04	0
Correlation coefficient	0.996	0.996	0.999
RMSE	0.16	0.29	0.24

are the registered counts of the eight detectors and the outputs are the positions coordinates (x,y,z) of the radioactive particle. As mentioned in section 3.1, only counts of the region corresponding to the photoelectric absorption were used as inputs of the ANN. In Fig. 4, it is shown the PHD of four detectors of the plane P1 (z = 0 cm) with the photopeak area highlighted in red to the position (0,9,0) of the radioactive particle.

The PHD was divided into 80 channels of 10 keV each. The counts related to the total absorption was in the 67th channel. For a better presentation, the ANN structure is arranged in Fig. 5.

4. Results and discussions

The results presented in this section are the processed data from the trained ANN to predict the instantaneous radioactive particle position inside the PVC tank for two distinct situations: i) air filled tank; ii) tank filled with concrete. Simulations were performed with the MCNPX code, using the tally card F8 for PHD results, but only the photoelectric absorption area was used to generate the results. The computer used to run the ANN was an Intel Core i5-4690 CPU @ 3.50 GHz and 16.0 GB of RAM. The ANN training time was approximately 2 min for the filled air tank and for the tank filled with concrete.

The optimized setup of a feed-forward multilayer perceptron with three hidden layers generated the best results. The ANN parameters, such as activation functions, learning rate and momentum, are given in Table 2.

4.1. Air filled tank

The coordinates x and y obtained by ANN in comparison to the MCNPX input data are shown in Fig. 6. Results are related to the training and test sets.

The results from the training and test sets show that the ANN follows the pattern from the simulations with MCNPX code. For a better evaluation of the results of the ANN, a minimum squares method was applied to a linear fit to correlate coordinates x and y from MCNPX code with ANN. The linear fit of the coordinates x and y is shown in Fig. 7. Correlation coefficient near 1 for all cases indicates a good convergence of the ANN.

Correlation coefficient (r^2) for training set is 0.999 for x and y coordinates. In the test set, for x-coordinate $r^2 = 0.997$ and for y-coordinate $r^2 = 0.991$. Results indicate a good compatibility between data generated by MCNPX and ANN.

The validation set is an important step because the ANN shows its potential to recognize new patterns that were not used in the training (learning) set. The final evaluation the off-line phase is shown in Fig. 8 and represents the coordinates x and y of the ANN in comparison with MCNPX.

It is possible to observe the tendency of ANN to follow the coordinates values given by the simulation with MCNPX code. To complete the evaluation of the validation set, the linear fit is shown in Fig. 9.

Correlation coefficient (r^2) from the linear fit for y-coordinate is

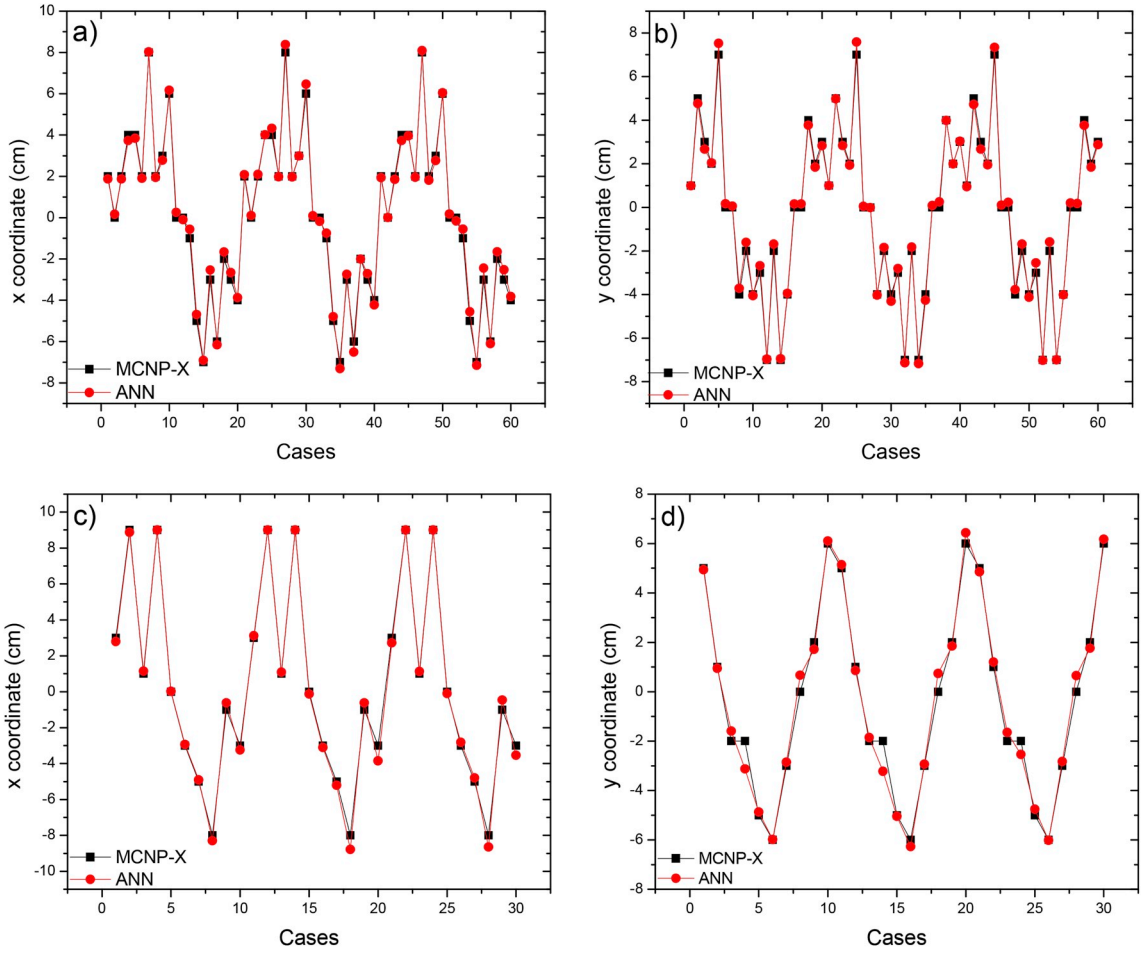

Fig. 11. Results for the tank filled with concrete comparing MCNPX with ANN: a) x-coordinate of training set; b) y-coordinate of training set; c) x-coordinate of test set; d) y-coordinate of test set.

0.993 and it shows that the ANN is converging well. For x-coordinate, $r^2 = 0.972$, which is also a good indicative of the ANN convergence. These results indicate a good acceptance of the proposed methodology.

As the z-coordinate has been varied in only three positions (z = 0 cm, z = −12.5 cm, z = −25 cm), the results for the learning (training and test sets) and validation sets are presented separated in Fig. 10. The results show a good convergence of the ANN and it indicates that the ANN could be capable to predict the z-coordinate as well.

The root mean square error (RMSE) is used to evaluate the ANN models by summarizing the differences between simulated data (MCNPX code) and predicted data (ANN). RMSE is calculated through Equation 2:

$$RMSE = \sqrt{\frac{\sum_{i=1}^{N} (x_{MCNPX} - x_{ANN})^2}{N}}$$

Where N is the total number of positions; x_{MCNPX} is the position simulated with MCNPX code; and x_{ANN} is the predicted position by the ANN. Important parameters to evaluate the ANN are relative errors, RMSE and the correlation coefficient, which evaluate the convergence of the ANN. The processed data generated by the ANN is shown in Table 3.

Analyzing the processed data, $r^2 = 0.99$ for all cases shows a good convergence of the ANN for the three coordinates. Over 60% of the results for x and y coordinates were below 5% of relative error. Meanwhile, for the z coordinate, over 90% were below 5% of relative error. Few cases above 30% of relative error, for all cases, are also a good parameter to evaluate the good convergence of the ANN.

4.2. Tank filled with concrete

The coordinates x and y obtained by ANN in comparison to the MCNPX data are shown in Fig. 11. These results are related to the learning phase (training and test sets).

It is possible to observe that ANN follows the pattern stipulated by the MCNPX code. To verify that, a minimum square method was applied to a linear fit function to evaluate the coordinates x and y comparing the results from the ANN with the results from the MCNPX code. The linear fit from the learning phase is shown in Fig. 12.

In the training set, the correlation coefficient (r^2) is 0.996 to the x coordinate and 0.997 to the y coordinate. In the test set, r^2 is 0.997 to the x coordinate and 0.987 to the y coordinate. The r^2 near 1 indicates convergence of the ANN.

The final evaluation of the ANN is the validation set, with cases that were not included in the learning phase. Coordinates x and y from MCNPX in comparison with ANN are shown in Fig. 13.

Comparing coordinates x and y generated in the MCNPX code with the response of the ANN, it is possible to observe a good compatibility

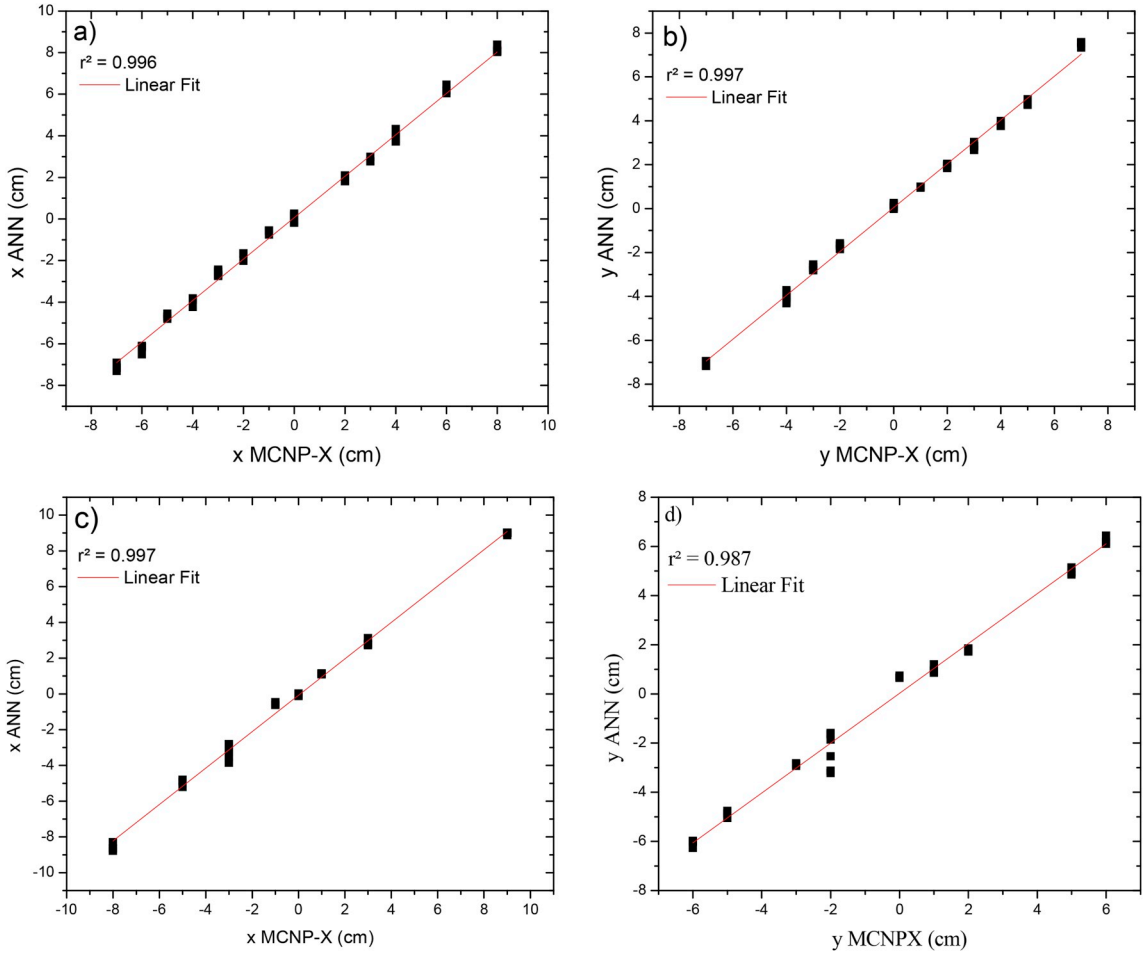

Fig. 12. Linear fit results for the tank filled with concrete: a) x-coordinate of the training set; b) y-coordinate of the training set; c) x-coordinate of the test set; d) y-coordinate of the test set.

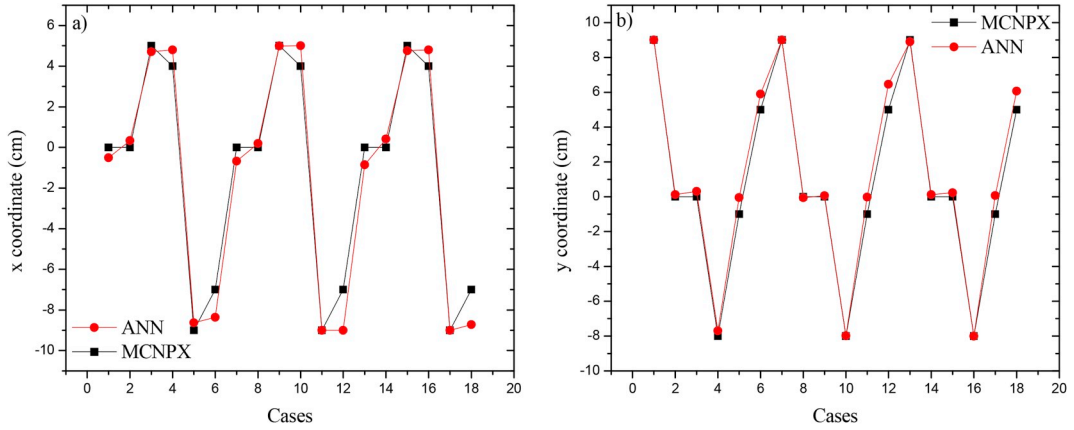

Fig. 13. Results of the validation set for the tank filled with concrete comparing MCNPX with ANN: a) x-coordinate; b) y-coordinate.

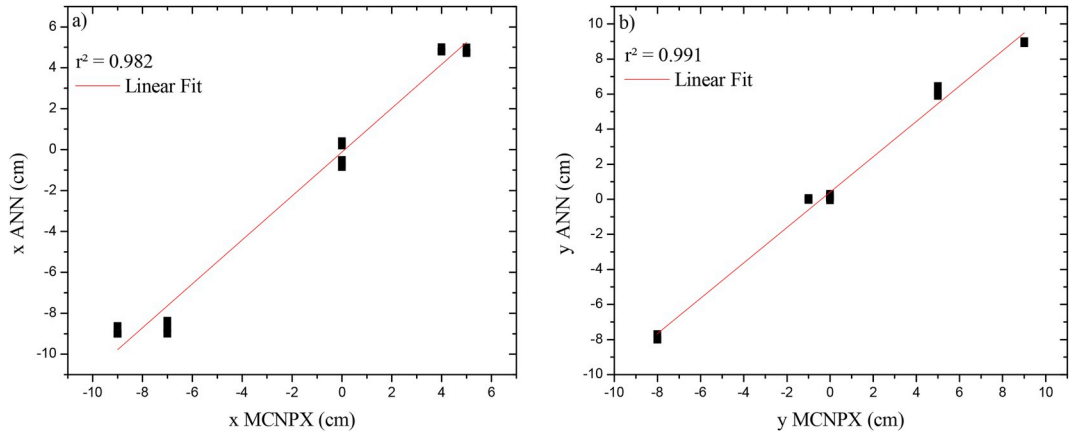

Fig. 14. Linear fit results of the validation set for the tank filled with concrete: a) x-coordinate; b) y-coordinate.

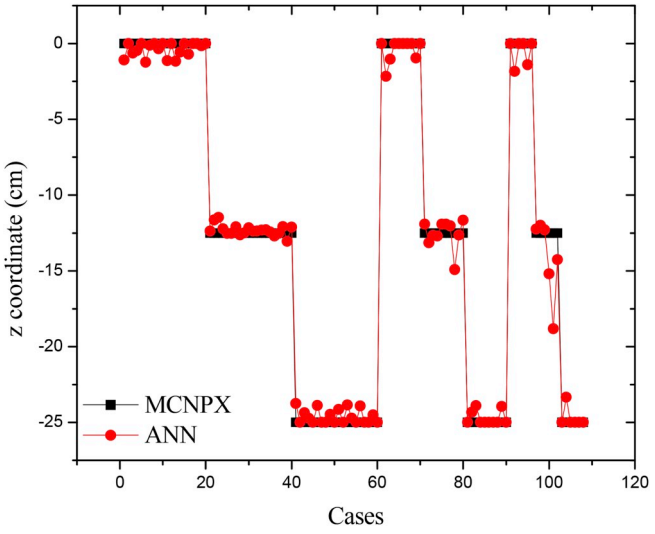

Fig. 15. Results of the z-coordinate for training, test and validation sets for the tank filled with concrete.

Table 4
Processed data from the trained ANN for the tank filled with concrete.

Processed data	Coordinates		
Relative Error	x	y	z
< 5%	48.89	50.72	87.50
5%–10%	26.67	22.99	6.94
10%–20%	11.11	13.79	2.78
20%–30%	7.78	6.90	1.39
> 30%	5.56	5.75	1.39
Correlation coefficient	0.996	0.996	0.996
RMSE	0.41	0.38	1.74

of the data. To confirm the results, the linear fit to coordinates x and y for the validation set are shown in Fig. 14.

The validation set has shown a r^2 for the x coordinate of 0.982, while for the y coordinate, the r^2 is 0.991. These results indicate that the ANN is converging well. It is important to point out that the validation set has fewer cases than the training and the test sets.

Similar to the simulation where the tank was filled with air, in this case, the z coordinate also varied in three positions only. Fig. 15 shows the z coordinate comparing to the MCNPX code and the ANN. It is possible to observe that the ANN results indicate a good compatibility with the data generated by MCNPX.

Analyzing the processed data in Table 4, $r^2 = 0.996$ for all cases shows a good convergence of the ANN for the three coordinates. Over 70% of the results for x and y coordinates were below 10% of relative error. Meanwhile, for the z coordinate, over 87% were below 5% of relative error. Few cases above 30% of relative error, for all cases, are also a good parameter to evaluate the good convergence of the ANN.

Fig. 16 presents the relative error for each position of the radioactive particle for coordinates x and y, to better view the information in Table 4.

In order to evaluate the radioactive particle trajectory inside the industrial mixer, Fig. 17 presents the comparison between positions (x,y) predicted by the ANN with the positions generated with MCNPX input data. It is important to notice that the positions were manually connected, so it is possible to evaluate the arbitrary trajectory of the radioactive particle.

These results indicated that the ANN is able to follow the movement of the radioactive particle within an industrial agitator.

5. Conclusions

In this work, it is presented a non-invasive methodology, based on the principles of the radioactive particle tracking technique, to predict the instantaneous position of the radioactive particle to monitor an industrial mixer. The modeling was performed by MCNPX code, and the reconstruction algorithm to locate the radioactive particle is given by a 3-layer feedforward artificial neural network with a backpropagation algorithm.

The results presented by the trained network, for air and concrete, indicates its great potential to predict the instantaneous position P (x,y,z) of the radioactive particle inside a volume of interest. For the tank filled with air, over 60% of the cases were below 5% of relative error for x and y coordinates. For z-coordinate, over 90% of the cases were below 5% of relative error. For the tank filled with concrete, over 70% of the cases were below 10% of relative error. For z-coordinate, over 87% of the cases were below 5% of relative error. The correlation coefficients (r^2) were 0.99 for both materials. These results also indicated that the methodology here presented could be a good diagnosis tool for industrial units. It is important to point out that this methodology does not need the use of large amount of calibration data and the network is able to converge with only 108 radioactive particle positions inside the concrete industrial mixer.

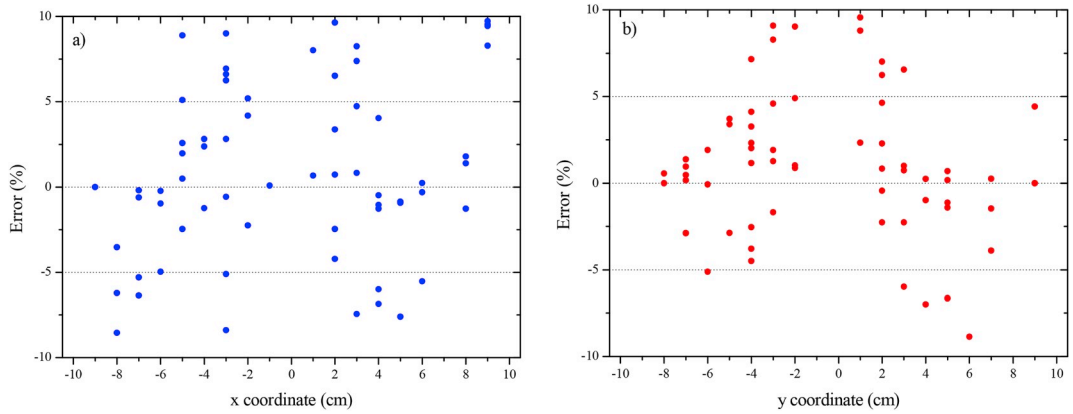

Fig. 16. Relative errors of the radioactive particle positions for: a) x-coordinate; b) y-coordinate.

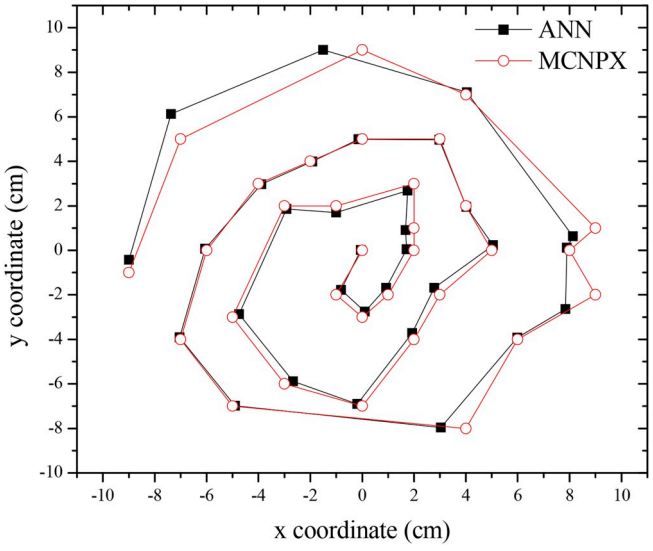

Fig. 17. Positions (x,y) predicted by the ANN in comparison with the positions generated by the MCNPX input data for the tank filled with concrete.

Acknowledgments

This study was financed in part by the Coordenação de Aperfeiçoamento de Pessoal de Nível Superior - Brasil (CAPES) - Finance Code 001. The authors gratefully thank the Instituto de Engenharia Nuclear (IEN) and Comissão Nacional de Energia Nuclear (CNEN) of Brazil.

References

Bhusarapu, S., Al-Dahhan, M.H., Dudukovic, M.P., Trujillo, S., O'Hern, T.J., 2005. Experimental study of the solids velocity field in gas–solid risers. Ind. Eng. Chem. Res. 44 (25), 9739.

Blet, V., Berne, P., Legoupil, S., et al., 2000. Radioactive tracing as aid for diagnosing chemical reactors. Oil Gas Sci. Technol. Rev. IFP 55 (2), 171–183.

Chaouki, J., Larachi, F., Dudukovic, P., 1997. Non-Invasive Monitoring of Multiphase Flows. Elsevier Science B.V, Amsterdam, The Netherlands.

Chauvin, Y., Rumelhart, D.E., 1995. Back-propagation Theory, Architectures and Applications.

Dam, R.S.F., Salgado, C.M., 2017. Study of the radioactive particle tracking technique using gamma-ray attenuation and mcnp-x code to evaluate industrial agitators. In: Annals of International Nuclear Atlantic Conference, Belo Horizonte, Brazil. XIII ENAN.

Devanathan, N., Moslemian, D., Dudukovic, M.P., 1990. Flow mapping in bubble columns using CARPT. Chem. Eng. Sci. 45, 2285–2291.

Doucet, J., Bertrand, F., Chaouki, J., 2008. An extended radioactive particle tracking method for systems with irregular moving boundaries. Powder Technol. 181 (2), 195–204.

Godfroy, L., Larachi, F., Kennedy, G., Grandjean, B., Chaouki, J., 1997. On-line flow visualization in multiphase reactors using neural networks. Appl. Radiat. Isot. 48, 225–235.

Haykin, S., 1999. Neural Networks, A Comprehensive Foundation, second ed. Prentice Hall.

Larachi, F., Kennedy, G., Chaouki, J., 1994. A gamma-ray detection system for 3-D particle tracking in multiphase reactors. Nucl. Instrum. Methods Phys. Res. Sect. A Accel. Spectrom. Detect. Assoc. Equip. 338 (2–3), 568–576.

Luo, H., Kemoun, A., Al-Dahhan, M.H., Sevilla, J.M.F., Sanchez, J.L.G., Camacho, F.G., Grima, E.M., 2003. Analysis of photobioreactors for culturing high-value microalgae and cyanobacteria via an advanced diagnostic technique: CARPT. Chem. Eng. Sci. 58 (12), 2519.

McConn Jr., R.J., Gesh, C.J., Rucker, R.A., Williams II, R.G., 2011. Compendium of Material Composition Data for Radiation Transport Modeling. PNNL-15870, Rev. 1. Pacific Northwest National Laboratoy.

Mosorov, V., Abdullah, J., 2011. MCNP5 code in radioactive particle tracking. Appl. Radiat. Isot. 69, 1287–1293.

Otawara, K., Fan, L., Tsutsumi, A., Kuramoto, K., Yoshida, K., 2002. An artificial neural network as a model for chaotic behavior of a three-phase fluidized bed. Chaos, Solit. Fractals 13, 353–362.

Parker, D.B., 1985. Learning Logic: Casting the Cortex of the Human Brain in Silicon. TR-47, M.I.T. Center for Computational Research in Economics and Management Science, Cambridge, MA Feb.

Pelowitz, D.B., 2005. MCNP-XMCNPX TM User's Manual. Version 2.5.0, LA-CP-05-0369. Los Alamos National Laboratory.

Roy, S., Larachi, F., Al-Dahhan, M.H., Dudukovic, M.H., 2002. Optimal design of radioactive particle tracking experiments for flow mapping in opaque multiphase reactors. Appl. Radiat. Isot. 56 (3), 485–503.

Rumelhart, D.E., McClelland, J.L., 1986. Parallel Distributed Processing, vol 1 MIT Press, Cambridge, MA.

Salgado, C.M., Brandão, L.E.B., Nascimento, C.M.N.A., Schirru, R., Ramos, R., Silva, A.X., 2009. Prediction of volume fractions in three-phase flows using nuclear technique and artificial neural network. Appl. Radiat. Isot. 67, 1812–1818.

Salgado, C.M., Pereira, C.M.N.A., Schirru, R., Brandão, L.E.B., 2010. Flow regime identification and volume fraction prediction in multiphase flows by means of gamma-ray attenuation and artificial neural networks. Prog. Nucl. Energy 52 (6), 555–562.

Tsoulfanidis, N., 1983. Measurement and Detection of Radiation. Series in Nuclear Engineering McGraw-Hill.

Werbos, P., 1974. Beyond Regression: New Tools for Prediction and Analysis in the Behavioral Sciences. Thesis of D.Sc. Harvard University, Cambridge, MA.

Yunos, M.A.S.M., Usang, M.D.A., Ithnin, H., Hussain, S.A., Yusoff, H.M., Sipaun, S., 2018. Reconstruction algorithm of calibration map for RPT techniques in quadrilateral bubble column reactor using MCNPX code. Eur. J. Eng. Res. Sci. 3 (1).

Zadeh, E.E., Feghhi, S.A.H., Roshani, G.H., Rezaei, A., 2016. Application of artificial neural network in precise prediction of cement elements percentages based on the neutron activation analysis. Eur. Phys. J. Plus 131, 167.

List of Acronyms

Al –: Aluminum
ANN –: Artificial neural network
MCNPX –: Monte Carlo N-Particle eXtended
MgO –: Magnesium oxide
NaI(Tl) –: Sodium iodide doped with thallium
PHD –: Pulse height distribution
PVC –: Polyvinyl chloride
RPT –: Radioactive particle tracking